European Journal of Radiology 117 (2019) 132–139

Contents lists available at ScienceDirect

European Journal of Radiology

journal homepage: www.elsevier.com/locate/ejrad

Research article

Multiparametric MR imaging to assess response following neoadjuvant systemic treatment in various breast cancer subtypes: Comparison between different definitions of pathologic complete response

G Santamaría[a,*], X Bargalló[a], S Ganau[a], I Alonso[b], M Muñoz[c], M Mollà[d], PL Fernández[e], A Prat[c]

[a] Department of Radiology, Institution of Hospital Clinic de Barcelona, Villarroel 170, 08036, Barcelona, Spain
[b] Department of Gynecology and Obstetrics, Institution of Hospital Clinic de Barcelona, Villarroel 170, 08036, Barcelona, Spain
[c] Department of Medical Oncology, Institution of Hospital Clinic de Barcelona, Villarroel 170, 08036, Barcelona, Spain
[d] Department of Radiation Oncology, Institution of Hospital Clinic de Barcelona, Villarroel 170, 08036, Barcelona, Spain
[e] Department of Pathology, Institution of Hospital Clinic de Barcelona, Villarroel 170, 08036, Barcelona, Spain

ARTICLE INFO

Keywords:
Magnetic resonance imaging
Breast cancer
Diffusion weighted MRI
Neoadjuvant treatment

ABSTRACT

Objectives: To validate the performance of multiparametric magnetic resonance (MR) imaging to assess pathologic response to neoadjuvant systemic therapy (NST) in various breast cancer subtypes considering two definitions of pCR: absence of any residual invasive cancer or DCIS (ypT0) and absence of invasive tumour cells (ypT0/is).

Methods: Institutional review board–approved retrospective study, with waiver of the need to obtain informed consent. From January 2015 to June 2017, 81 women with 82 breast cancers undergoing NST were included. Eighteen lesions (22%) were immunohistochemically HER2-positive, 12 (15%) triple negative (TN), 42 (51%) luminal B-like and 10 (12%) luminal B-like/HER2-positive. Breast MR imaging was performed before and after NST. A comparative analysis considering pCR as ypT0 and ypT0/is was carried out. Performance of univariate and multivariate models to potentially predict pathologic response were evaluated.

Results: ypT0 was attained in 23% (19/82) of cases and ypT0/is in 33% (27/82) of cases. In both scenarios, HER2-positive subtype achieved the best response, 53% and 48%, respectively. A significant relationship was found between late enhancement and pathologic response ($p < 0.001$) regardless of pCR definition. In the ypT0 scenario, mean ADC ratio in the pCR subgroup was significantly higher than that in the non-pCR subgroup ($p = 0.021$) but no significant relationship was noted in ypT0/is. A multivariate model including MR late enhancement, ADC ratio and tumor subtype identified pathologic response with 86% and 84% accuracy when ypT0 and ypT0/is were considered, respectively.

Conclusion: MR imaging late enhancement and ADC ratio along with breast cancer IHC subtype identify pathologic response following NST with high accuracy, achieving the highest NPV in TN and HER2-positive tumors and the highest PPV in luminal B-like subtypes, regardless of the definition of pCR as ypT0 or ypT0/is. In light of these findings and given that residual DCIS does not have an impact on survival rates, ypT0/is seems to be the preferable definition of pCR.

1. Introduction

The approach to breast cancer management radically changed with the advent of the new classification of breast cancer intrinsic subtypes based on gene expression patterns [1,2]. Concurrently, neoadjuvant systemic treatment (NST) has become a well-established treatment option even in early-stage breast cancer as it has been shown that pathologic complete response (pCR) after NST is significantly related to better long-term survival in most of the cancer subtypes [3–5]. Recent improvements in neoadjuvant therapies have led to increasing rates of pCR which has motivated an emerging interest in the possibility of avoiding surgery in selected groups of patients [6–8].

Magnetic resonance (MR) imaging has become paramount in the monitoring of response to NST [9] as it has been shown to reliably assess the treatment performance, when compared with other imaging modalities such as mammography or ultrasound [9,11]. The predictive value of various parameters detected on dynamic contrast-enhanced (DCE) MR imaging and diffusion imaging has been reported [12–15]

* Corresponding author at: Present address: Translational Research Institute (TRI), 37 Kent Street, Woolloongabba, QLD, 4102, Australia.
E-mail address: gorane.santamaria@tri.edu.au (G. Santamaría).

https://doi.org/10.1016/j.ejrad.2019.06.009
Received 9 December 2018; Received in revised form 10 May 2019; Accepted 11 June 2019

but the lack of consensus regarding the definition of pCR makes it difficult to identify which MR imaging findings are the mainstay to predict pathologic response following NST. Furthermore, the combination of specific antimitotic and nonspecific antiangiogenic effects of taxane-containing chemotherapy has an impact on the accuracy of DCE MR imaging in predicting pCR [16]. In this regard, in a previous study, our group reported a significant association of late enhancement and ADC ratio with pathologically response after neoadjuvant treatment, especially in HER2-positive and triple-negative (TN) tumors [17]. Other studies have also shown that delayed sequences in the posttreatment MR imaging are more accurate than early sequences for evaluating residual disease [18].

The purpose of the study is to validate the performance of multiparametric MR imaging to assess pathologic response following NST according to our previous work, now comparing two definitions of pCR: absence of any residual invasive cancer or DCIS (ypT0) and absence of invasive tumour cells (ypT0/is).

2. Materials and methods

2.1. Patients selection

This is a single institutional review board-approved retrospective study with waiver of the need to obtain informed consent.

Women with luminal B-like, HER2-positive or triple-negative biopsy-proven breast cancers who were scheduled to undergo NST were included in the study. Luminal A-like cancers were excluded as these tumors do not respond to chemotherapy and pCR is not expected in this patient collective.

A simplified classification based on immunohistochemistry (IHC) of estrogen receptor (ER), progesterone receptor (PR), human epidermal growth factor 2 (HER2) and Ki67 was used to identify the intrinsic subtypes. Thus, breast cancers were divided into 4 different IHC groups: TN (*i.e.* ER-negative, PR-negative and HER2-negative), HER2-positive (*i.e.* ER-negative, PR-negative and HER2-positive), luminal B-like (*i.e.* ER-positive or PR-positive, HER2-negative and Ki67 ≥ 14%) [19] and luminal B-like/HER2+ (*i.e.* ER-positive or PR-positive and HER2-positive).

All cancer subtypes received a multi-agent chemotherapy regimen consisting of epirubicin and cyclophosphamide for 12 weeks (at three-weely intervals), followed by weekly paclitaxel for 12 weeks. Additionally, HER2-positive tumors received trastuzumab in combination with paclitaxel prior to surgery.

2.2. MR imaging technique

Breast MR imaging, including contrast-enhanced MR imaging and echo planar diffusion-weighted (DW) imaging, was performed prior to the start of NST and following completion of treatment, at most 2 weeks prior to definitive surgical excision.

MR equipment included: a) 1.5-T MR imaging system (Signa, GE medical Systems, Milwaukee, USA) with a dedicated bilateral four-channel breast surface coil and, b) 1.5-T MR imaging system (Aera, Siemens, Erlangen, Germany) with a dedicated bilateral sixteen-channel breast surface coil. Table 1 shows the summary of sequence parameters in both magnets. All patients were imaged in prone position as per the protocol described elsewhere [17]. Pretreatment and posttreatment MR imaging were performed in the same magnet for each patient. For the dynamic study, the bolus injection consisted of 0.1 mmol gadobutrol (Gadovist; Bayer, Berlin, Germany) per kilogram of body weight and a 20-mL saline flush, delivered through an intravenous cannula inserted in an antecubital vein.

2.3. MR imaging interpretation

Three radiologists, with 20, 13 and 10 years of experience interpreted breast MR imaging independently using a dedicated workstation (GE Healthcare, Advantage Windows 4.4). Each patient had their pretreatment and posttreatment MR imaging reported by the same radiologist. No interobserver agreement was assessed. In turn, the reporting radiologist was treated as a variable in the model to predict pathologic response.

Tumor response to treatment was assessed using the Response Evaluation Criteria in Solid Tumors (RECIST 1.1) classification [20], based on the longest diameter measure of the target lesion. Likewise, any change in tumor vascularity between both dynamic MR imaging examinations was also assessed. Two types of tumor enhancement were described: early enhancement, observed 72 or 75 s after contrast administration depending on the magnet (Table 1) and, late enhancement, observed 360 or 375 s after contrast administration. Late enhancement was treated as a categorical variable (absent/present).

According to these criteria, three possible radiologic responses were identified in the posttreatment MRI: (a) radiologic complete response, complete absence of both early and late enhancement; (b) radiologic partial response, partial disappearance of early enhancement in the lesion or complete absence of early enhancement but persistence of late enhancement; and (c) no radiologic response, including stable or progressive disease [17].

For the largest target lesion, the apparent diffusion coefficient (ADC) value was measured before and after NST. A single ROI (≥20 mm [2]) was set by the radiologist in one of the most representative tumor slices, avoiding the inclusion of surrounding parenchyma and areas of necrosis. The ADC value obtained from that single ROI was the one used for subsequent analyses. Whenever a radiologic complete response was achieved after treatment, we compared the pretreatment and posttreatment MR imaging and looked for anatomical references to find the site where the tumor was located in the first place so that the ROI was properly placed where the tumor was meant to be. For data analysis, ADC ratio (posttreatment ADC/ pretreatment ADC) was calculated [17].

Table 1
Parameters of MR imaging sequences.

DWI sequence (EPI)	SIGNA	AERA
TR (ms)	8000	6500
TE (ms)	65	66
Slice thickness (mm)	4	4
FoV (mm)	320 × 320	360 × 270
Matrix (mm)	132 × 132	192 × 115
b values (s/mm^2)	0/700	50/700
T2 FSE sequence		
TR	3800	1200
TE	120	253
Slice thickness	2	2
FoV	330 × 330	340 × 340
Matrix	416 × 416	512 × 476
3D T1-weighted sequence		
Flip angle	15º	10º
TR	4.7	4.65
TE	2.3	1.78
Slice thickness	2	2
FoV	330 × 330	340 × 340
Matrix	416 × 416	416 × 416
In-plane resolution (mm)	0.8 × 0.8	0.8 × 0.8
Acquisition time (sec)	72	75

EPI: echo-planar imaging; TR: Repetition time; TE: Echo time; FoV: Field of view.

2.4. Histopathologic assessment

Tumor features were obtained from histopathologic reports of core biopsies performed prior to NST. The analysis was performed by a pathologist with 27 years of experience (PLF). The histologic type and

Table 2
Clinical, pathologic and imaging findings according to different definitions of pCR (ypT0 and ypT0/is).

	ypT0			ypT0/is		
	Non responders (n = 63)	Responders (n = 19)	p value	Non responders (n = 55)	Responders (n = 27)	p value
Age (years)			< 0.001			0.003
Mean ± SD	59 ± 12	50 ± 8		60 ± 12	52 ± 10	
Range	38-85	40-65		38-85	40-81	
Histologic type			ns			ns
Ductal	54 (86)	17 (90)		46 (84)	25 (93)	
Lobular	4 (6)	0		4 (7)	0	
Other	5 (8)	2 (10)		5 (9)	2 (7)	
Histologic grade[a]			ns			0.050
1	6 (10)	1 (5)		6 (12)	1 (4)	
2	35 (60)	9 (47.5)		31 (62)	13 (48)	
3	17 (30)	9 (47.5)		13 (26)	13 (48)	
Breast cancer IHC subtype[b]						
Triple negative	8 (13)	4 (21)	0.045	7 (13)	5 (18)	0.076
Her2-positive	8 (13)	10 (53)	< 0.001	5 (9)	13 (48)	< 0.001
Luminal B-like	38 (60)	4 (21)		34 (62)	8 (30)	
Luminal B-like/Her2-positive	9 (14)	1 (5)		9 (16)	1 (4)	
Posttreatment axillary status			0.013			0.001
Negative	40 (66)	18 (92)		33 (61)	25 (96)	
Positive	21 (34)	1 (8)		21 (39)	1 (4)	
Mean tumor size ± SD (mm)	30.7 ± 14.5	37.4 ± 18.5	ns	29.5 ± 12.4	38 ± 20	ns
Late enhancement in posttreatment MRI			< 0.001			< 0.001
Absent	8 (13)	11 (58)		6 (11)	13 (48)	
Present	55 (87)	8 (42)		49 (89)	14 (52)	
Mean pretreatment ADC ± SD (mm^2/s)	1.070 ± 0.248	1.063 ± 0.219	ns	1.059 ± 0.256	1.091 ± 0.205	ns
Mean posttreatment ADC ± SD (mm^2/s)	1.513 ± 0.398	1.733 ± 0.352	0.037	1.515 ± 0.412	1.663 ± 0.351	ns
Mean ADC ratio ± SD	1.440 ± 0.411	1.725 ± 0.480	0.021	1.465 ± 0.424	1.580 ± 0.471	ns

Data in parentheses are percentages.

[a] ypT0: Percentages calculated for 58 cancers in the non-responder subgroup and for 19 cancers in the responder subgroup with histologic grade available. ypT0/is: Percentages calculated for 50 cancers in the non-responder subgroup and for 27 cancers in the responder subgroup with histologic grade available. Grades 1 and 2 were considered in the same category for statistical analysis.

[b] Considering luminals B-like as the reference IHC subtype. IHC = immunohistochemical, SD: standard deviation, ADC = apparent diffusion coefficient.

grade were recorded. HER2 status positivity was defined as a 3+ score by IHC. Equivocal cases at IHC (2+ score) were subjected to silver in situ hybridization analysis. The assessment of ER and PR status were carried out by IHC according to the current guidelines [21]. Ki-67 proliferation marker was also assessed.

Breast surgical specimens were fixed in 10% neutral-buffered formalin, paraffin embedded, sectioned and stained with hematoxylin and eosin (H&E) for evaluation.

Histopathologic analysis was the gold standard to assess pathologic response which was classified into: a) complete disappearance of the tumor (only residual fibrosis noted), b) presence of DCIS and, c) presence of invasive carcinoma.

For analysis purposes, two different definitions of pCR were applied: complete absence of any residual invasive cancer or DCIS (ypT0) and absence of invasive cells in the breast specimen (ypT0/is).

The pathologist was blinded to the MR imaging results. Where disagreement existed between MR imaging studies and pathologic findings, radiological findings were reassessed along with the pathologist to identify any reasons for discrepancy.

2.5. Statistical analysis

Tumor IHC subtype, maximum lesion size measured on pretreatment MR imaging (mm), posttreatment axillary status, reporting radiologist, presence or absence of MR imaging-detected late enhancement, ADC ratio, histologic type, histologic grade and pathologic response were collected.

Chi-squared test or Fisher exact test were used as appropriate to compare categorical variables. Intergroup mean comparison of ADC ratios was performed using Kruskal-Wallis test for several groups comparison. Univariate and multivariate logistic regression analyses was performed to determine if any variables were predictive of pCR as ypT0 or ypT0/is. Adequate receiver operating characteristic (ROC) curves were built to evaluate the diagnostic accuracy of the models. A two-sided p-value of < 0.05 was considered statistically significant. Statistical analysis was undertaken by using IBM SPSS Statistics for Windows, Version 20.0 (IBM, Armonk, NY).

3. Results

3.1. Patients

A total of 81 women with 82 pathologically proven invasive breast cancer undergoing NST were included (mean age, 57 years; age range, 38–85).

3.2. Histopathologic and IHC features of breast cancers

According to the IHC subtype, 42 tumours were luminal B-like, 10 were luminal B-like/HER2 positive, 18 were HER2-positive and the remaining 12 were TN.

When it comes to the histologic type, 87% (71/82) of cancers were ductal type, 5% (4/82) were lobular and the remaining 7 were other types.

Regarding the histologic grade, 9% (7/77) were grade 1, 57% (44/77) were grade 2 and 34% (26/77) were grade 3. The pathologist did not report the grade in lobular tumors and in one papillary cancer.

The mean pre-treatment tumour size measured by MRI was 29 mm (SD: 14) for the luminal B-like subtype, 35 mm (SD: 23) for luminal B-like/HER2-positive, 30 mm (SD: 12) for HER2-positive and 44 mm (SD: 17) for triple-negative cancers (p = 0.033).

Mean Ki-67 was 28% (SD: 12) for the luminal B-like subtype, 28% (SD: 14) for luminal B-like/HER2-positive, 40% (SD: 23) for HER2-positive and 53% (SD: 28) for TN (p = 0.027).

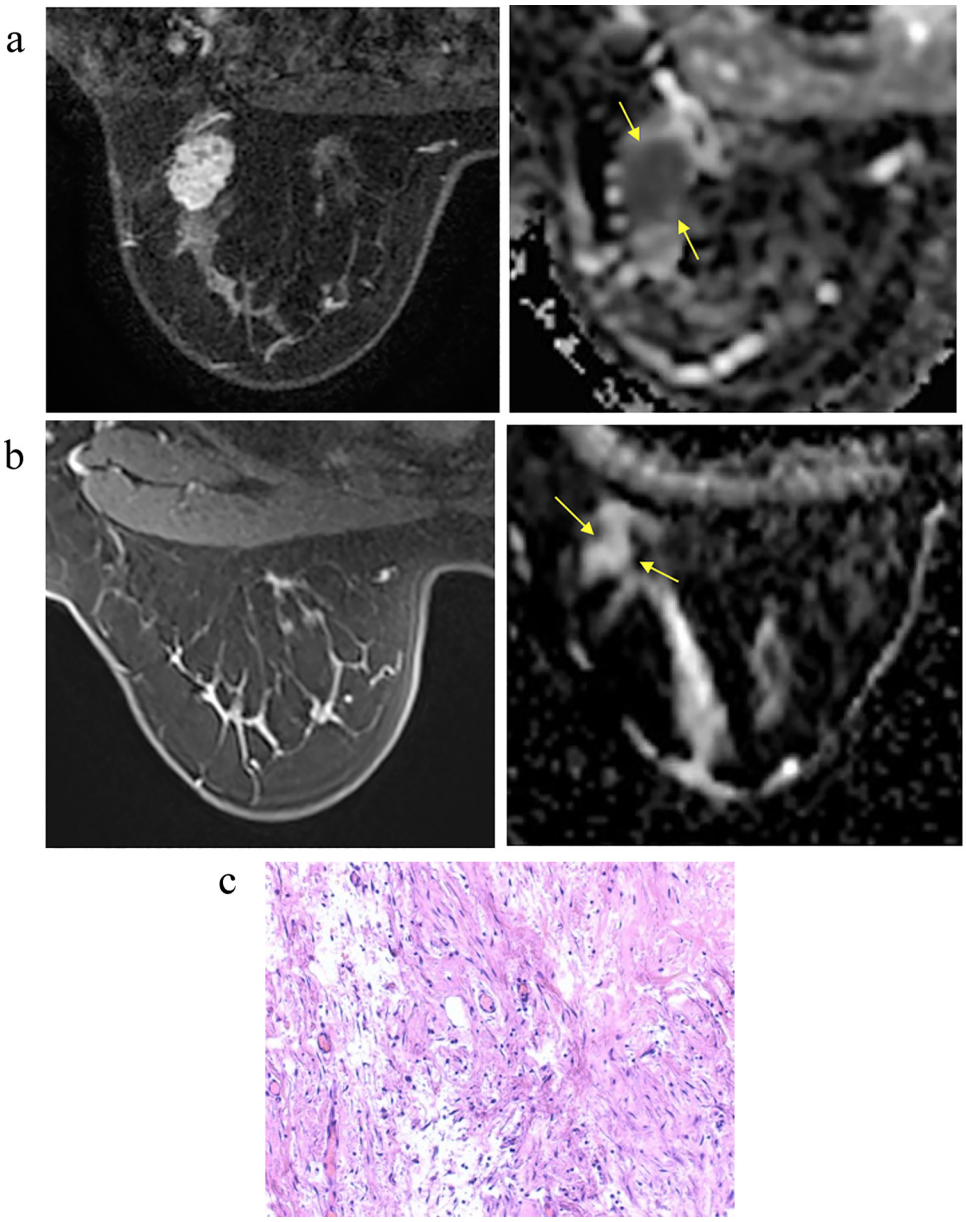

Fig. 1. 44-year-old woman with HER2-positive breast cancer.
a) Left: Axial pretreatment T1-weighted dynamic MR imaging (72 s after gadolinium injection) shows a lobulated mass enhancement in the lateral and posterior aspect of the right breast corresponding to breast cancer.
Right: Axial diffusion- weighted imaging. ADC map shows restricted diffusion within the mass (arrows) (ADC: 0.876 mm^2/s).
b) **Left**: Axial posttreatment T1-weighted dynamic MR imaging (375 s after gadolinium injection). Note absence of enhancement in the tumor bed in late sequence.
Right: Diffusion-weighted imaging. ADC map. A hyperintense area (arrows) is noted in the region where the lesion was detected before NST (ADC: 1.463 mm^2/s). ADC ratio: 1.670. Radiologic complete response was reported and pCR predicted.
c) Microphotograph shows pCR. Extensive fibrotic area in the tumor bed with no residual neoplasia (H&E, x100).

Clinical, pathologic, and radiologic findings of responders and non-responders according to different definitions of pCR are shown in Table 2.

ypT0 was achieved in 23% (19/82) of the cases. Ten out of these (53%) were HER2-positive tumors (Fig. 1), 5/19 (26%) were included in the luminal B-like and Luminal B-like/ HER2-positive subtypes and the remaining 4/19 (21%) were TN.

ypT0/is was identified in 33% (27/82) of the cases that included the previously described 19 cases plus 8 with residual DCIS. Three out of these residual DCIS (38%) were observed in HER2-positive tumors, 4/8 (50%) were included in the luminal B-like and Luminal B-like/ HER2-positive subtypes and the remaining case (12%) was TN.

At the time of diagnosis, 43% (35/82) of the cases had axillary metastases. Of these, 37% (13/35) achieved ypN0 after treatment. Six out of 13 (46%) were HER2-positive, 4/13 (31%) TN and 3/13 (23%) luminal B-like. Seven out of 13 (54%) also achieved ypT0 in the breast (4 HER2-positive, 2 TN and 1 luminal B-like) whereas in the remaining cases no breast complete response was reported ($p = 0.192$).

Ninety-five percent (21/22) of axillary metastases after NST were recorded in the non- responders subgroup both for ypT0 and ypT0/is (Table 2).

3.3. Contrast-enhanced MR imaging and DW imaging findings

Late enhancement in posttreatment MR imaging was observed in a higher proportion of non-responders than responders for both definitions of pCR ($p < 0.001$) (Table 2).

The average ADC ratio of the series was 1.499 (SD: 0.438) with no significant differences across subtypes ($p = 0.484$).

When pCR was considered as ypT0, the mean ADC ratio was significantly higher in complete responders than in non-responders ($p = 0.021$) (Table 2). Posttreatment late enhancement was present in 77% (63/82) of the cases. Eight out of these 63 cases (13%) showed late enhancement but ypT0 was reported in all of them. The histopathologic examination of these false-positive (FP) cases revealed inflammatory changes associated to NST (Fig. 2) in 5 cases, usual hyperplasia in 2 cases and fibrocystic changes in 1 case. Three of these FP cases were TN, 3 were HER2-positive and 2 were luminal B-like. ADC ratio was higher than the mean ADC ratio value in all TN and in two HER2-positive cases with a range between 1.770 and 2.639. One out of the

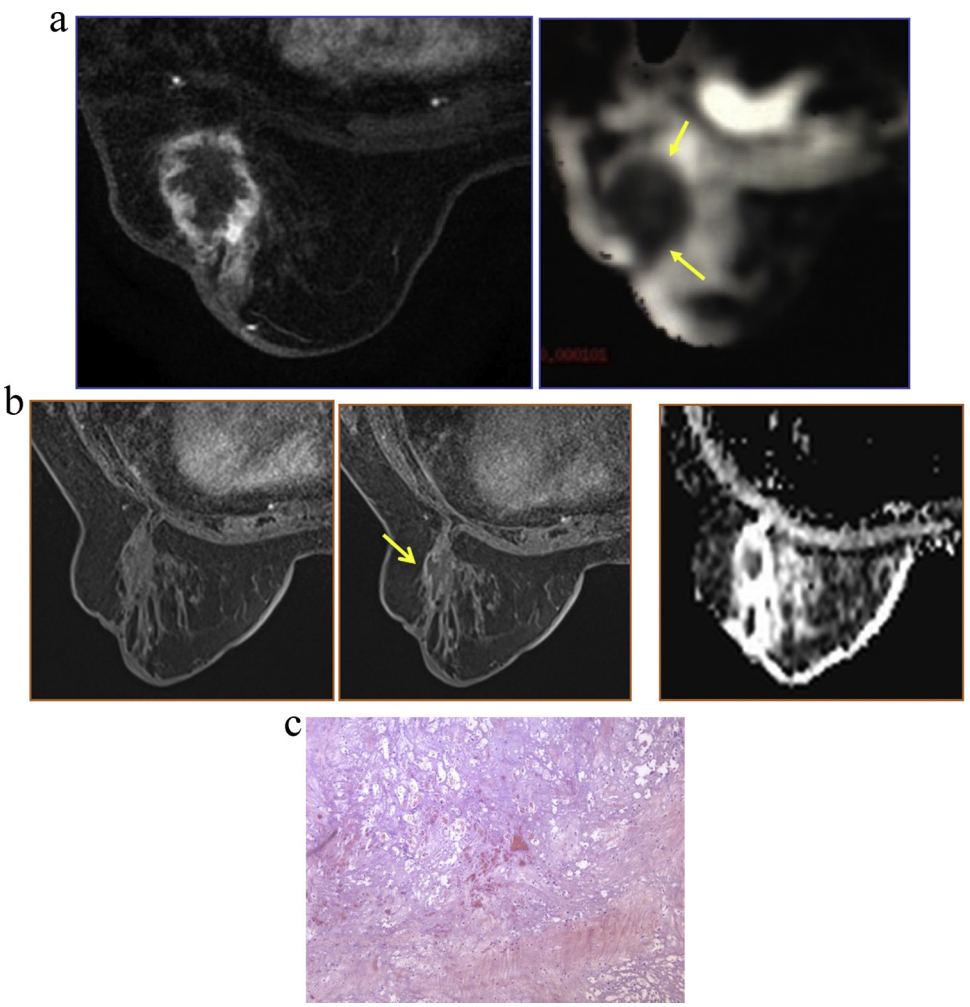

Fig. 2. 65-year-old woman with triple-negative breast cancer.
a) **Left**: Axial pretreatment T1-weighted dynamic MR imaging (72 s after gadolinium injection). A lobulated with partially irregular margins mass enhancement is seen in the right breast. Note the rim enhancement due to tumoral necrosis within the lesion.
Right: Axial diffusion-weighted imaging. ADC map. The area corresponding to the breast cancer shows hypointensity (arrows) meaning restricted diffusion because of the high tumor cellularity.
b) **Left**: Axial posttreatment T1-weighted dynamic MR imaging (75 s after gadolinium injection) shows no remarkable enhancement in the early sequence.
Middle: Note the subtle peripheral tumor enhancement (arrow) in the late sequence (375 s after gadolinium injection).
Right: Axial ADC map shows hyperintensity in the tumor bed. ADC ratio was 2.489. In spite of this high value suggesting complete response, the subtle enhancement was assessed as a likely residual tumor.
c) Microphotograph shows pCR (H&E, x40). Granulation tissue and fibrosis are seen. No residual cancer is identified. Granulation tissue disclosed some vessels (not shown), likely responsible for the enhancement identified on MR imaging.

HER2-positive and the luminal B-like tumors exhibited lower than the average ADC ratios with a range between 1.310 and 1.480.

A cut-off ADC ratio value of 1.701 was found to classify patients into pCR and non pCR with 82% specificity (18% FP) and 56% sensitivity.

In the same scenario, absence of late enhancement on posttreatment MR imaging was reported in 23% (19/82) of tumors. Of these, 58% (11/19) achieved pCR. There were, however, 42% (8/19) of patients who demonstrated absence of late enhancement but did not achieve pCR. Histopathologic examination of these false-negative (FN) cases showed DCIS in two of them (one HER2-positive and 1 luminal B-like) and isolated tumor cells immersed in a large fibrotic stroma in the remainder of the cases (Fig. 3). Seven of the FN cases were luminal-like tumors (5 luminal B-like, 2 luminal B-like/Her2+) and 1 case was HER2-positive. ADC ratio was under the average in 7 out of 8 cases with a range between 1.030 and 1.498. Only one of the luminal B-like cancers demonstrated an ADC ratio of 1.532.

When pCR was considered as ypT0/is, the two previously described cases with residual DCIS became true negatives whereas the remaining 6 cases with residual DCIS were FP as all of them showed late enhancement.

Table 3 shows the performance of posttreatment MR late enhancement to identify pathologic response in various tumor IHC subtypes in both pCR scenarios. In ypT0, the highest sensitivity to detect residual tumor was in the TN subtype (100%) followed by HER2-positive tumors with 88% sensitivity and relatively high specificity (70%). The highest specificity was identified in the luminal B-like/HER2-positive subtype (100%). Likewise, the highest positive predictive value (PPV) was recorded in luminal B-like subtypes whereas negative predictive value (NPV) was higher in TN and HER2-positive tumors. These results were comparable to those obtained in pyT0/is, except for a better sensitivity and NPV (100%) in HER2+ and a moderately higher NPV (43%) in luminal B-like tumours in the ypT0/is scenario.

3.4. ROC Analyses

Table 4 summarizes the univariate and multivariate models to assess the performance of MR late enhancement, ADC ratio and IHC subtype to potentially predict pathologic response. The best model to predict ypT0 includes the three variables, thus achieving 86% diagnostic accuracy (95% CI: 74%, 99%).

When ypT0/is was considered as pCR, the ROC analyses did not improve the results obtained in the ypT0 scenario as seen in Table 4. Moreover, ADC ratio was not significantly related to prediction of ypT0/is and multivariate model including ADC ratio and late enhancement overlapped with that including late enhancement alone. On the contrary to ypT0, no ADC cut-off value could be identified in ypT0/is as there was no significant relationship between ADC ratio and pathologic response in the univariate model.

Compared to luminal B-like subtypes, ypT0 was almost 12 times more frequent in HER2-positive tumors and nearly 5 times more frequent in TN cancers. Likewise, the probability of ypT0 was 4 times higher per unit increase in the ADC ratio. Conversely, the presence of late enhancement in the posttreatment MR imaging decreased the probability of ypT0 (OR: 0.106).

No significant relationship was identified between the reporting radiologist and the prediction of ypT0 or ypT0/is.

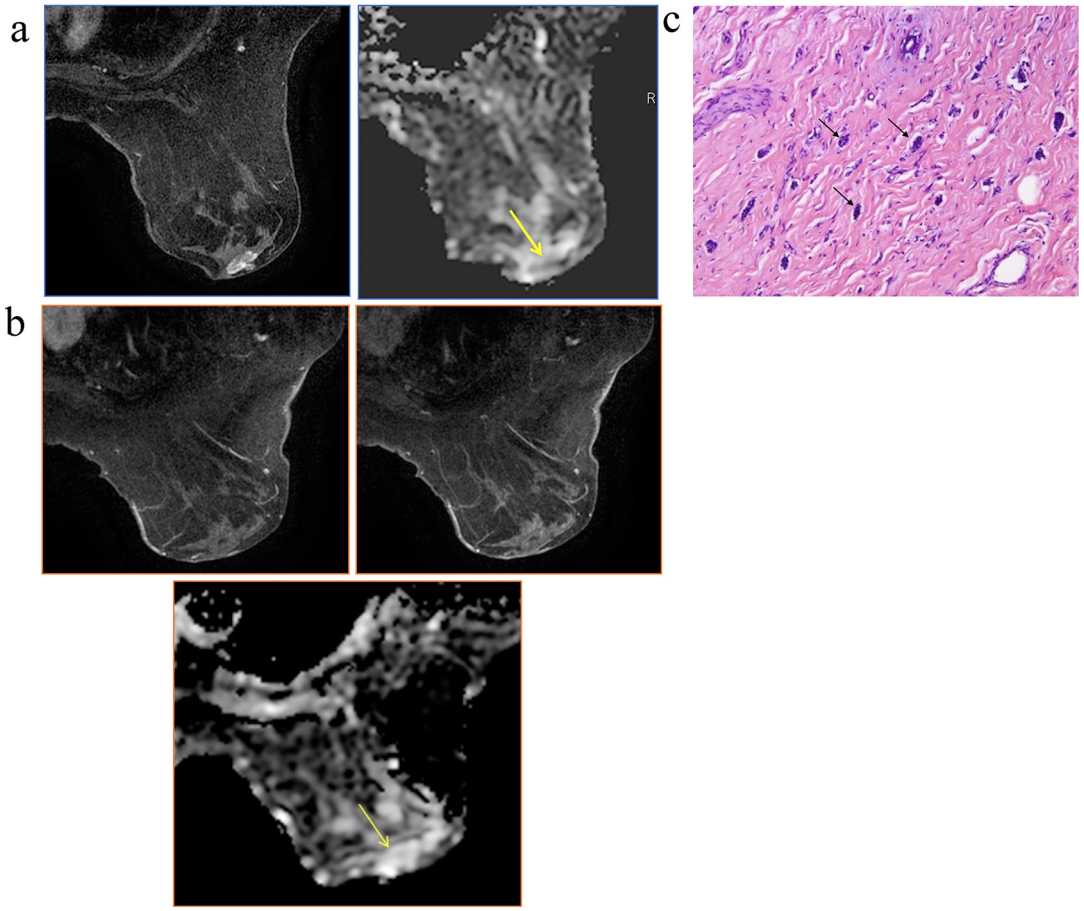

Fig. 3. 67-year-old woman with luminal B-like breast cancer.
a) **Left**: Axial pretreatment T1-weighted dynamic MR imaging (72 s after gadolinium injection) shows a retroareolar circumscribed mass enhancement in the left breast.
Right: Axial ADC map shows hypointensity in the tumor region (arrow) due to restricted diffusion.
b) **Superior**: Axial posttreatment T1-weighted dynamic MR imaging in early (72 s after gadolinium injection) (left) and late (360 s after gadolinium injection) (right) sequences shows no remarkable enhancement in the retroareolar area favouring radiologic complete response.
Inferior: Axial ADC map shows hyperintensity in the tumor bed (arrow) suggesting complete response to NST. However, ADC ratio was 1.401 (under the average).
c) Microphotograph shows isolated tumoral cells (arrows) immersed in an extensive fibrotic area (H&E, x100).

Table 3
Performance of MR late enhancement to predict pathologic response according to different definitions of pCR.

	ypT0					ypT0/is				
	Luminal B-like	Luminal B-like/HER2+	Triple Negative	HER2+	Overall	Luminal B-like	Luminal B-like/HER2+	Triple negative	HER2+	Overall
Sensitivity[a]	87 (33/38)	78 (7/9)	100 (8/8)	88 (7/8)	87 (55/63)	88 (30/34)	78 (7/9)	100 (7/7)	100 (5/5)	89 (49/55)
Specificity[b]	50 (2/4)	100 (1/1)	25 (1/4)	70 (7/10)	58 (11/19)	38 (3/8)	100 (1/1)	20 (1/5)	62 (8/13)	48 (13/27)
PPV[c]	94 (33/35)	100 (7/7)	73 (8/11)	70 (7/10)	87 (55/63)	86 (30/35)	100 (7/7)	64 (7/11)	50 (5/10)	78 (49/63)
NPV[d]	29 (2/7)	33 (1/3)	100 (1/1)	88 (7/8)	58 (11/19)	43 (3/7)	33 (1/3)	100 (1/1)	100 (8/8)	68 (13/19)

[a] Sensitivity: correct identification of residual tumor.
[b] Specificity: correct identification of pCR.
[c] PPV: positive predictive value.
[d] NPV: negative predictive value.

4. Discussion

Our results confirm that MR imaging late enhancement and ADC ratio along with breast cancer IHC subtype identify pathologic response following NST with high accuracy achieving the highest negative predictive value in TN and HER2-positive tumors, regardless of the definition of pCR as ypT0 or ypT0/is. The easy availability of these three parameters allows the practical application of this potential predictive model in the clinical setting. These results are in line with those previously reported by our group [17], thus confirming the potential of multiparametric MRI to accurately predict pCR.

In the neoadjuvant setting, pCR needs to be predicted with high accuracy and a low FN rate. There are several reasons that help explain FN cases in the NST setting. These issues are related to (a) definition of pCR, (b) type of chemotherapy regimen, (c) different behavior of breast cancer subtypes undergoing NST.

The disparity of results among studies highlights the need for agreement in terms of pCR definition, as it has significant implications

Table 4
Performance of univariate and multivariate models to predict pathologic response after NST according to different definitions of pCR.

	ypT0		ypT0/is	
	ODDS RATIO	AUC (CI 95%)	ODDS RATIO	AUC (CI 95%)
Late enhancement	0.106	0.73 (0.58–0.87)	0.132	0.69 (0.56–0.82)
ADC ratio	4.002	0.69 (0.54–0.84)		NA[a]
Tumor subtype		0.76 (0.63–0.89)		0.75 (0.63–0.87)
HER2 positive	11.750		12.422	
Triple negative	4.700		3.413	
Luminal B-like				
ADC ratio and tumor subtype		0.78 (0.65–0.92)		0.76 (0.63–0.90)
Late enhancement and tumor subtype		0.84 (0.73–0.95)		0.81 (0.70–0.92)
Late enhancement and ADC ratio		0.80 (0.65–0.95)		NA
Late enhancement, ADC ratio, tumor subtype		0.86 (0.74–0.99)		0.84 (0.73–0.95)

[a] NA: not applicable.

on both prognosis and therapeutic decision-making. In our study, two definitions of pCR were considered and compared. ypT0 was achieved in 23% of cases whereas ypT0/is was attained in 33% of cases. Kaise et al [22] documented pCR in 12.3% of cases with a restrict definition of complete response as absence of any type of cancer whereas NSABP B-27 [23] reported pCR in 26% of cases, including DCIS in this category. Our results show that in the ypT0/is scenario the multivariate model including the three above mentioned variables attains 84% accuracy to potentially predict pCR. This means a slight decrease in accuracy compared to that achieved when considering ypT0 (86%), but, in contrast, a 100% sensitivity and 100% NPV is achieved in HER2-positive tumours aside from the same high values in TN. Therefore, as DCIS in the surgical specimen after NST does not have an impact on outcomes, including disease-free and overall survival rates [24], it seems reasonable to consider ypT0/is as a preferable definition of pCR, as Choi et al [25] recently concluded.

Regarding the axillary status, most of the cases showing axillary metastases after treatment were included in the non-responder breast subgroup. Likewise, most of the ypN0 were achieved in HER2-positive and TN cancers, meaning that these cancer subtypes respond much better to NST not only in the breast but also in the axillary lymph nodes. Kim et al [26] reported that tumor response rate of the breast cancer was the most significant independent predictor of axillary pCR in response to neoadjuvant chemotherapy which is in line with our own results.

When it comes to the type of chemotherapy regimen, it is known that as a consequence of taxane-containing neoadjuvant chemotherapy, a decrease in tumor vascularity and permeability of the tumour microvasculature is expected [16]. These changes affect the delivery of MR contrast agent into the lesion and thereby leading to underestimation of residual disease [27]. The aim of MR imaging delayed sequences in the neoadjuvant setting is to allow the contrast agent to reach the tumor in order to identify MR late enhancement, which is mostly related to residual disease [17]. Therefore, delayed sequences following contrast administration allow to better identify the pathologic response and reduce the FN rate. In a recent publication, Kim et al [18] also found that in the post neoadjuvant setting, conventional delayed-phase MRI (360 s after contrast administration) is more accurate than early-phase MRI (90 s after contrast administration) to evaluate residual breast tumor size. In our study, this procedure lead to an overall PPV of 87% and 78% when ypT0 and ypT0/is were considered, respectively. Note should be made, however, that dynamic MRI fails to detect some small residual DCIS or isolated invasive cells after NST, even if delayed sequences are used. In this regard, this issue would not have an impact whether ypT0/is was considered as pCR. Moreover, the FN cases related to non-enhancing DCIS would drop, thus increasing the NPV which, in our study, amounts to an overall 68%.

In the ypT0 scenario, ADC ratio plays an important role in assessing pathologic response in these FN cases. We observed that when no delayed enhancement was identified and low ADC ratio values were recorded, pCR was less likely to happen than in cases where ADC ratio was above average.

Finally, the varying behavior of breast cancer subtypes on chemotherapy may also help explain the FN rate. Our study showed that in ypT0, posttreatment MRI reached an overall 58% NPV, but a breakdown by subtypes demonstrates a different behavior among them. Thus, TN or HER2-positive tumors achieve 100% and 88% NPV, respectively whereas luminal B-like tumors reach a poor 29% NPV. Loo [28] also concluded that MRI to monitor response to NST was effective in TN or HER2-positive tumors but inaccurate in luminal subtypes. Likewise, the systematic review by Lobbes [10] reported that cancer subtype can influence MRI accuracy and should be considered in clinical decision-making. It is essential that radiologists take into account the breast cancer subtype when reporting posttreatment MRI, as this will likely lead to a reduction in the number of FN and FP cases. Most of FP cases were TN and HER2-positive which exhibited very high ADC ratios, an indirect sign of response to NST [17]. Furthermore, we identified 1.701 as a tentative ADC ratio cut-off value to classify cases into ypT0 and non-responders achieving 82% specificity even if the sensitivity was low (56%). In this regard, although in our previous work [17] we ventured that most responders had ADC ratios higher than 1.5, we could not get a proper cut-off value. This could have likely been due to the fact that the classification by subtypes was done differently, *e.g.* all luminal subtypes were included in the same group and all cancers showing HER2-positive, even if they were luminal, were part of the same group. On the contrary, in the present study, aside from luminal A-like cancers being excluded, we split HER2-positive tumors into those showing ER-negative, PR-negative and those with luminal features, thus better defining the different subtypes.

There are some limitations in the study. First, it is a single-institution retrospective study with a limited number of patients. Second, the variability by magnet type was not included in the analysis. The results, however, do reinforce the ability of multiparametric MR imaging to assess pathologic response in the neoadjuvant setting whatever the pCR definition.

In conclusion, the present study confirms that MR imaging late enhancement and ADC ratio along with breast cancer IHC subtype identify pathologic response following NST with high accuracy, achieving the highest NPV in TN and HER2-positive tumors and the highest PPV in luminal B-like subtypes, regardless of the definition of pCR as ypT0 or ypT0/is. In light of these findings and given that residual DCIS does not have an impact on survival rates, ypT0/is seems to be the preferable definition of pCR. Validation of these findings in larger prospective studies would support the utility of multiparametric MRI, which might identify patients who require additional therapies or excellent responders in whom breast cancer surgery could even be avoided.

Aleix Prat´s conflicts of interest

- Novartis Farmaceútica, S.A.–Advisory Role, Research Support
- Roche Farma, S.A. –Advisory Role, Research Support
- Lilly Spain–Advisory Role
- Pfizer, S.L.U–Advisory Role
- Oncolytics Biotech Inc Scientific–Advisory Role
- Bristol-Myers Squibb, S.A.U. –Advisory Role
- Amgen, S.A. –Advisory Role
- Sysmex Europe GmbH–Research Support
- Medical Scientia Inno. –Research, S.L Research Support
- Celgene, SLU–Research Support
- Astellas Pharma, S.A. –Research Support
- Nanostring Technologies–Research Support

There are no other conflicts of interest.

References

[1] C.M. Perou, T. Sorlie, M.B. Eisen, et al., Molecular portraits of human breast tumors, Nature 406 (2000) 747–752.

[2] A. Prat, C. Perou, Deconstructing the molecular portraits of breast cancer, Mol. Oncol. 5 (2011) 5–23.

[3] F. Peintinger, W.F. Symmans, A.M. Gonzalez-Angulo, et al., The safety of breast-conserving surgery in patients who achieve a complete pathologic response after neoadjuvant chemotherapy, Cancer 107 (2006) 1248–1254.

[4] J. Cuzik, T. Powles, U. Veronesi, et al., Overview of the main outcomes in breast-cancer prevention trials, Lancet 361 (2003) 296–300.

[5] G. Minckwitz, M. Untch, J.U. Blohmer, et al., Definition and impact of pathologic complete response on prognosis after neoadjuvant chemotherapy in various intrinsic breast cancer subtypes, J. Clin. Oncol. 30 (2012) 1796–1804.

[6] M.E.M. van der Noordaa, F.H. van Duijnhoven, C.E. Loo, et al., Identifying pathologic complete response of the breast after neoadjuvant systemic therapy with ultrasound guided biopsy to eventually omit surgery: study design and feasibility of the MICRA trial (minimally invasive complete response assessment), Breast 40 (2018) 76–81.

[7] R.F.D. van La Parra, H.M. Kuerer, et al., Selective elimination of breast cancer surgery in exceptional responders: historical perspective and current trials, Breast Cancer Res. (2016), https://doi.org/10.1186/s13058-016-0684-6.

[8] H.M. Kuerer, G.M. Rauch, S. Krishnamurthy, et al., A clinical feasibility trial for identification of exceptional responders in whom breast cancer surgery can be eliminated following neoadjuvant systemic therapy, Ann. Surg. (2017), https://doi.org/10.1097/SLA.0000000000002573.

[9] M.L. Marinovich, N. Houssami, P. Macaskill, et al., Meta-analysis of magnetic resonance imaging in detecting residual breast cancer after neoadjuvant therapy, J. Natl. Cancer Inst. 105 (2013) 321–333.

[10] M.B.I. Lobbes, R. Prevos, M. Smidt, et al., The role of magnetic resonance imaging in assessing residual disease and pathologic complete response in breast cancer patients receiving neoadjuvant chemotherapy: a systematic review, Insights Imag. 4 (2013) 163–175.

[11] Y. Gu, S.M. Pan, J. Ren, Z.X. Yang, G.Q. Jiang, Role of magnetic resonance imaging in detection of pathologic complete remission in breast cancer patients treated with neoadjuvant chemotherapy: a meta-analysis, Clin Breast Canc 17 (2017) 245–255.

[12] L. Minarikova, W. Bogner, K. Pinker, et al., Investigating the prediction value of multiparametric magnetic resonance imaging at 3 T in response to neoadjuvant chemotherapy in breast cancer, Eur. Radiol. 27 (2017) 1901–1911.

[13] A. Fangberget, L.B. Nilsen, K.H. Hole, et al., Neoadjuvant chemotherapy in breast cancer-response evaluation and prediction of response to treatment using dynamic contrast-enhanced and diffusion-weighted MR imaging, Eur. Radiol. 21 (2011) 1188–1199.

[14] R. Woodhams, S. Kakita, H. Hata, et al., Identification of residual breast carcinoma following neoadjuvant chemotherapy: diffusion-weighted imaging comparison with contrast-enhanced MR imaging and pathologic findings, Radiology 254 (2010) 357–336.

[15] N.M. Hylton, C.A. Gatsonis, M.A. Rosen, et al., Neoadjuvant chemotherapy for breast cancer: functional tumor volume by MR imaging predicts recurrence-free survival results from the ACRIN 6657/CALGB 150007 I-SPY 1 TRIAL, Radiology 279 (2016) 44–55.

[16] S. Schrading, C. Kuhl, Breast cancer: influence of taxanes on response assessment with dynamic contrast-enhanced MR imaging, Radiology 277 (687) (2015) 696.

[17] G. Santamaría, X. Bargalló, P.L. Fernández, B. Farrús, X. Caparrós, M. Velasco, Neoadjuvant systemic therapy in breast cancer: association of contrast-enhanced MR imaging findings, diffusion-weighted imaging findings, and tumor subtype with tumor response, Radiology 283 (2017) 663–672.

[18] S.Y. Kim, N. Cho, I.A. Park, et al., Dynamic contrast-enhanced breast MRI for evaluating residual tumor size after neoadjuvant chemotherapy, Radiology 4 (2) (2018) 163–175.

[19] M.C.U. Cheang, S.K. Chia, D. Voduc, et al., Ki67 index, HER2 status, and prognosis of patients with luminal B breast cancer, J. Natl. Cancer Inst. 101 (2009) 736–750.

[20] E.A. Eisenhauer, P. Therasse, J. Bogaerts, et al., New response evaluation criteria in solid tumours: revised RECIST guideline (version 1.1), Eur. J. Cancer 45 (2009) 228–247.

[21] M.E. Hammond, D.F. Hayes, M. Dowsett, et al., American Society of Clinical Oncology/ College of American Pathologists guideline recommendations for immunohistochemical testing of estrogen and progesterone receptors in breast cancer, J. Clin. Oncol. 28 (2010) 2784–2795.

[22] H. Kaise, F. Shimizu, K. Akazawa, et al., Prediction of pathological response to neoadjuvant chemotherapy in breast cancer patients by imaging, J. Surg. Res. 225 (2018) 175–180.

[23] P. Rastogi, S.J. Anderson, H.D. Bear, et al., Preoperative chemotherapy: updates of national surgical adjuvant breast and bowel project protocols B-18 and B-27, J. Clin. Oncol. 26 (2008) 778–785.

[24] Mazouni Ch, F. Peintinger, S. Wan-Kau, et al., Residual ductal carcinoma in situ in patients with complete eradication of invasive breast cancer after neoadjuvant chemotherapy does not adversely affect patient outcome, J. Clin. Oncol. 25 (2007) 2650–2655.

[25] M. Choi, Y.H. Park, J.S. Ahn, et al., Evaluation of pathologic complete response in breast cancer patients treated with neoadjuvant chemotherapy: experience in a single institution over a 10-year period, J. Pathol. Transl. Med. 51 (2017) 69–78.

[26] H.S. Kim, M.S. Shin, C.J. Kim, et al., Improved model for predicting axillary response to neoadjuvant chemotherapy in patients with clinically node-positive breast cancer, J. Breast Cancer 20 (2017) 378–385.

[27] Y. Yuan, X.S. Chen, S.Y. Liu, K.W. Shen, Accuracy of MRI in prediction of pathologic complete remission in breast cancer after preoperative therapy: a meta-analysis, AJR Am. J. Roentgenol. 195 (2010) 260–268.

[28] C.E. Loo, M.E. Straver, S. Rodenhuis, et al., Magnetic resonance imaging response monitoring of breast cancer during neoadjuvant chemotherapy: relevance of breast cancer subtype, J. Clin. Oncol. 29 (2011) 660–666.